CFD ANALYSIS OF FIRE PROTECTION SPRINKLER SYSTEM ADAPTED FOR A STORAGE/SALE RACK OF FLAMMABLE LIQUIDS

Patricio Valdés Gacitúa

IDIEM - Investigación, Desarrollo e Innovación de Estructuras y Materiales
Plaza Ercilla 883
Santiago, Región Metropolitana, 8320000, Chile
e-mail: patricio.valdes@idiem.cl

ABSTRACT

This research was conducted to study and analyze if a sprinkler system designed by NFPA codes would be able to control or extinguish a fire on a storage/sale rack of flammable liquids.

The study was carried out through computational simulations in the CFD package denominated "Fire Dynamics Simulator" following the technical features of the flammable rack widely used in retail sale throughout several countries in Latin America and Europe.

The intention of the store where the units are installed was to study if a sprinkler system designed under NFPA 30 and NFPA 13 would be capable of controlling or extinguishing a fire produced in the flammable liquids part of the unit. Due to operational and commercial reasons, the racks do not fulfill any design codes such as NFPA 30. Therefore, the stated CFD analysis has been used as an instrument to demonstrate if the sprinkler system would work effectively (due to the unit's design) and, consequently, it could prevent incorrect fire protection designs.

For this study, a validation case scenario was assessed considering a real fire test in a flammable liquids rack to corroborate the fire propagation. Moreover, the sensitivity analysis was evaluated regarding the fire and sprinkler discharge to obtain the mesh cell size. Lastly, a scenario in which the burning flammable liquids unit interacts with the sprinkler system was analyzed, ultimately obtaining the performance of the sprinklers design.

As a result, it is possible to argue that the CFD analysis was used as an engineering tool to demonstrate that the adaptation of the design of a sprinkler system (proposed by the store), is incapable of controlling or extinguishing the fire in the flammable rack, since these units do not fulfill a design technical code.

Keywords: Flammable, liquids, rack, storage, sprinklers, FDS, NFPA 30, NFPA 13, Simulations, Fire, Full-scale test, CFD, thinners, paints, ethanol.

INTRODUCTION

A Chilean store sells different types of products in theirs stores, distributing and storing their products in different conditions. There is a particular fire safety concern for the management of the store, regarding to the combustible and flammable liquids (such as thinners, paints, white spirits, etc.) organized in racks and arranged for sale.

According to the store´s management, a fire full-scale test has been conducted to assess if the pre-engineered dry chemical system installed is able to extinguish a fire in the rack. The test conducted determined that the dry chemical system is not able to control or extinguish the fire. Due to the fire scale test results, the store´s management has decided to install an in-rack sprinkler solution according NFPA 30.

The store management indicates that a re-arrangement of the rack geometry or an exchange of the format to store flammable and combustible liquids (plastic bottles), it would impact negatively in the sales of the products. Therefore, the store´s management decision is to follow the NFPA 30 rules as much as possible without significantly impacting the racks or the plastic bottles. By this way, the sprinklers system designed will be an “adaptation” from the code to the existing racks.

Due to IDIEM is a technical advisor from the store´s management, it has indicated that the solution proposed by the store´s management does not fulfill important requirements of the code. Therefore, IDIEM has developed a CFD analysis of fire protection sprinkler system proposed by the store´s management, to demonstrate that the adaptation of the design is incapable of controlling or extinguishing the fire in the flammable rack, since these units do not fulfill a design technical code.

METHODOLOGY

The following methodology has been assessed in order to develop the present study.

Information Review

It's reviewed the information regarding to the stored flammable and combustible items in the rack, rack configuration, materiality, geometry, among others technical characteristics. In addition, the NFPA 30: Flammable and Combustible Liquids Code is reviewed to identify the requirements for the flammable storage.

Fire Full Scale Test Results

Due to the rack arrangement does not fulfill any code or regulation for flammable storage, a fire full scale test has been developed to:

- Test if the actual fire extinguishment system would control or extinguish a fire.
- Investigate the fire dynamics in the current rack arrangement.
- Represent a reliable CFD simulation of the fire dynamics in the flammable rack.

Sprinklers System Adaptation

Based on the rack configuration and the characteristics of the flammable containers, a sprinkler system designed based on NFPA 13 and NFPA 30 will be designed. Due to operational and commercial reasons, the arrangement of the rack and the vessels or containers of liquids do not fulfill any design codes such as NFPA 30. Thus, due to the store´s requirements, an adaptation of a sprinkler system will be designed, trying to fulfill the code as much as possible.

CFD Simulations

The CFD simulations will be computed in the FDS (Fire Dynamics Simulator) package. The rack arrangement, the fire and the interaction with the previously designed sprinkler system will be modeled in the CFD package.

In this chapter, the following topics are developed, to assess a reliable simulation:

- Performance evaluation
- Assumptions and considerations regarding with fire dynamics
- Fire scenarios
- Sensitivity analysis
- Modelling Configuration

INFORMATION REVIEW

The storage rack for combustible and flammable liquids is constructed of bolted metal profiles, with 7 storage levels (Figure 1). Each level contains two metal trays 1m deep x 1.25m wide and 0.1m height. The ground level has a height of 0.62m, and the consecutive levels are place at height of 0.44m (Figure 2). Each side of the rack is separated by 0.2m (Figure 4).

Figure 1: Real arrangement of the storage rack in the store

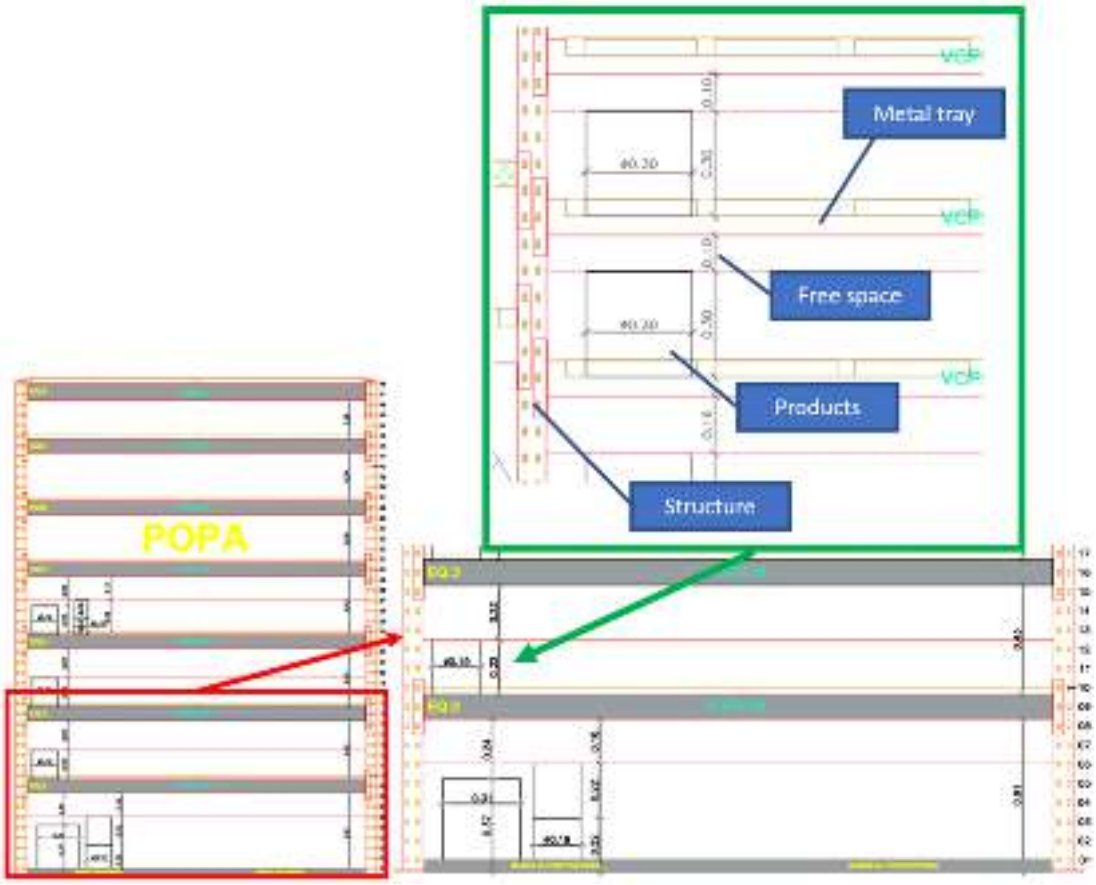

Figure 2: Elevation view of the storage rack

The first 4 rack of the complete storage store flammable materials described in the Table 1, while the rest of the racks store combustible products as water and oil-based paintings, leak sealant, neoprene-based adhesive, among others (Figure 4).

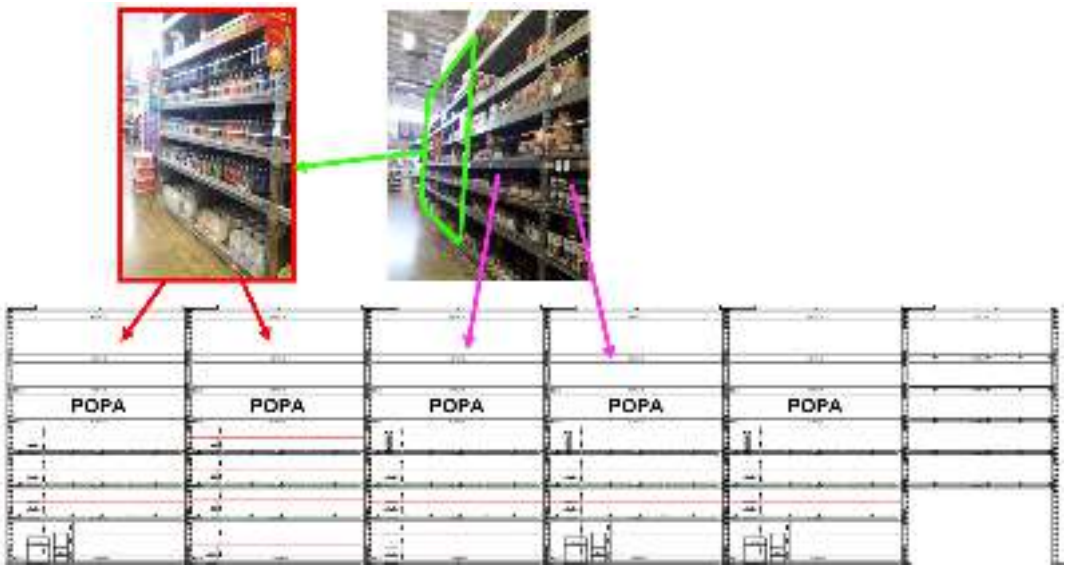

Figure 3: Organization of the flammable and Combustible products in the storage rack

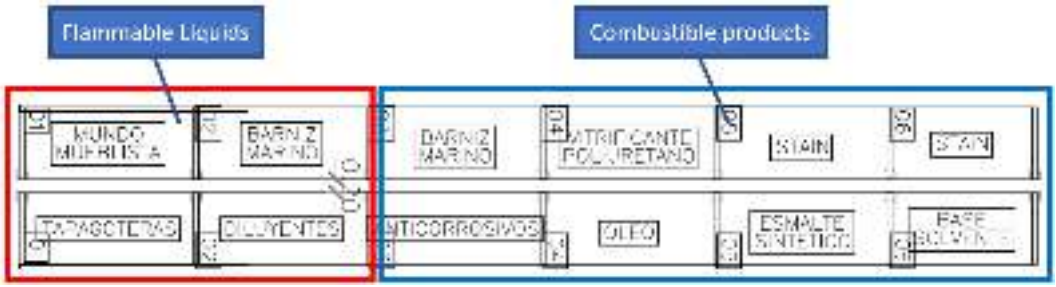

Figure 4: Plan view of the storage rack

The flash point and boiling point of the products are presented in the Table 1.

Table 1: Flash and boiling point for the liquids stored in the rack

Product	Flash point (°C)	Boiling point (°C)	Water Solubility
Synthetic thinner	< 0	255	Insoluble
White gasoline	< -18	288	Insoluble
Solvent	11	464	Miscible
Thinner	-3,3	535	Insoluble
Thinner type “duco”	-3,3	535	Insoluble
Polyurethane thinner	36	498	Insoluble
Pyroxylin thinner	-3,3	535	Insoluble
Acrylic thinner	-3,3	400	Insoluble
Solvent	11	464	Miscible
Thinner for pool paint	27	527	Insoluble
White spirit	38	275	Insoluble

FULL SCALE TEST RESULTS

The fire full scale test was conducted to obtain the following information:

- Test if the actual fire extinguishment system would control or extinguish a fire.
- Investigate the fire dynamics in the current rack arrangement.
- Represent a reliable CFD simulation of the fire dynamics in the flammable rack.

The arrangement of the rack to be tested is presented in the Figure 5, where it is possible to see the quantity and the display of the flammable liquids in the metal trays. The Figure 5 present the zone where the ignition point will be placed, considering the spill of 1 liter of white gasoline.

Figure 5: Arrangement of the rack

From T=0s until T=5s it is possible to see how the fire evolves from the ignition and then the spill continues burning.

At T=6s the fixed dry chemical system has triggered discharging the suppressor agent, but it does not any influence on the fire developing, as is possible to see at T=6s and T=10s. At T=11s the flames start to interact with the upper metal tray and the flammable liquids stored there, starting to burn them.

At T=16 due to the fire spreading and heating-up of the plastic containers, jet flames begin to be produced and fire keeps growing and spreading. The flame height reaches the fourth metal tray.

At T=20s it is possible to see that the flame height reaches the fifth metal tray, while the generated jet fires and the rupture of the plastic containers, start to spill flammable liquids into the ground. This behavior contributes with the fire growing and with the fire propagation downwards, igniting the flammable liquids in the first metal tray.

At T=24s all the metal trays are involved in fire, besides, the jet fire produced by the rupture of the plastic containers increases the fire severity and burning surface.

At T=27s the fire severity continuous increasing the fire as well burning surface. Currently, the fire service interrupts the test due to the severity of the fire.

Figure 6: Timeline of the full scale fire test conducted, including the dry chemical system.

SPRINKLER SYSTEM ADAPTATION

The main liquids stored in the racks correspond to Heptane, Methanol, Toluene, Isopropanol, Ethanol, among others. According to the NFPA 30 standard, it is possible to classify liquids as flammable and combustible (Figure 7).

4.3.1 Flammable liquids, as defined in 3.3.33.2 and 4.2.3, shall be classified as Class I liquids and shall be further subclassified in accordance with the following:

(1) Class IA Liquid — Any liquid that has a flash point below 73°F (22.8°C) and a boiling point below 100°F (37.8°C)
(2) Class IB Liquid — Any liquid that has a flash point below 73°F (22.8°C) and a boiling point at or above 100°F (37.8°C)
(3) Class IC Liquid — Any liquid that has a flash point at or above 73°F (22.8°C), but below 100°F (37.8°C)

4.3.2 Combustible liquids, as defined in 3.3.33.1 and 4.2.2, shall be classified in accordance with the following:

(1) Class II Liquid — Any liquid that has a flash point at or above 100°F (37.8°C) and below 140°F (60°C)
(2) Class III Liquid — Any liquid that has a flash point at or above 140°F (60°C)
   (a) Class IIIA Liquid — Any liquid that has a flash point at or above 140°F (60°C), but below 200°F (93°C)
   (b) Class IIIB Liquid — Any liquid that has a flash point at or above 200°F (93°C)

Figure 7: NFPA 30 Ed. 2012 – Art. 4.3.1 and Art. 4.3.2

Table 2: Liquids Classification

Liquid	Boiling Point (°C)	Flash Point (°C)	Classification
Methanol	64,7	12	IB
Ethanol	78,4	12,7	IB
Isopropanol	82,5	11,2	IB
Toluene	110	4,4	IB
Etan	98,4	-3,8	IB

The type of container currently used in the storage of combustible and flammable liquids corresponds to disposable light plastic bottles (Figure 8).

Figure 8: Liquid Bottles

Under the requirements of NFPA 30 standard – Art. 9.4 “Acceptable Containers”, it is possible to indicate that the current bottles do not meet the requirements of the NFPA 30 standard for "Plastic or Metal Containers" (Art. 9.4.1). This article indicates the standards or codes for the construction of the containers, bottles, recipients (among others) for storage petroleum products. Thus, according to NFPA 30 Handbook, very thin-walled plastic containers not intended for reuse (same as used in the actual configuration), should not be used for routinary and repeated storage of flammable products and combustible liquids.

The current rack configuration has characteristics that do not meet the construction requirements required by the NFPA 30 standard, due to there are not enough space that allow the generation of flue gases for the activation of the longitudinal flume sprinklers.

Therefore, the current racks do not fit in the category of fuel and flammable storage racks approved to be protected with automatic sprinklers. However, it is compatible with a retail aisle. Nevertheless, due to the client´s requirement and to explore the design of an appropriate extinguishing system for this type of installation, the protection is assimilated to one of "flammable liquids in rack storage".

As a result, the fire protection requirements indicated in NFPA 30 Ed. 2012 – Art.16.5, through the table 16.5.2.7, the arrangement of the sprinklers shall be as its shown in the Figure 9. The In-rack sprinkler system shall provide that the 8 most remote sprinklers operate at operating pressure of 50 psi, whereas the ceiling sprinklers shall be capable of discharge the density indicated in the Table 3.

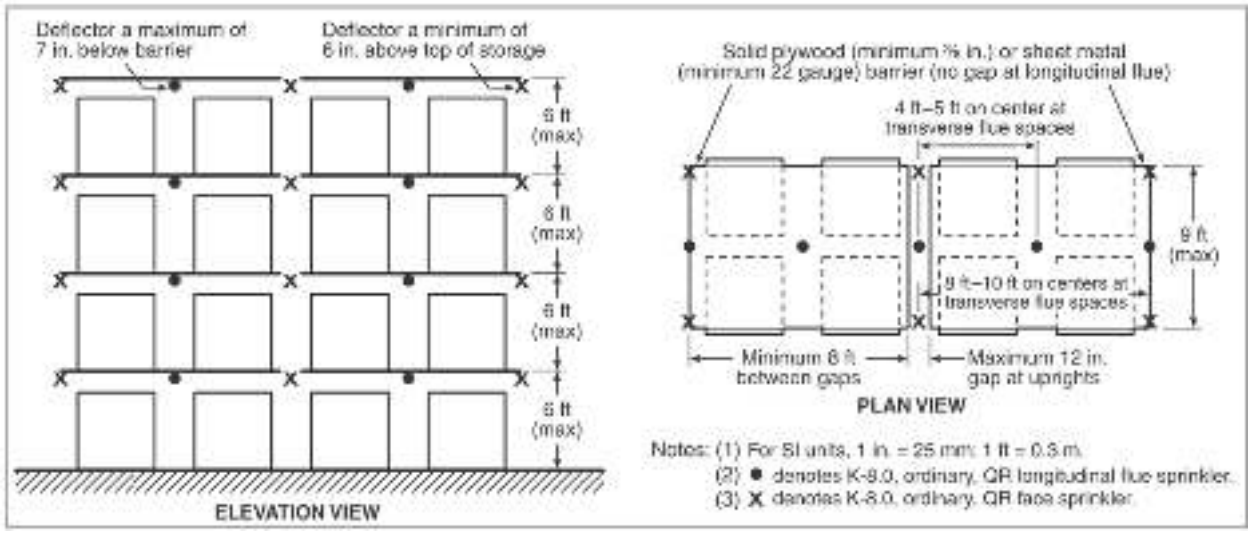

Figure 9

The requirements for the In-rack sprinklers and ceiling sprinklers according to NFPA 30 are shown in the Table 3.

Table 3: Sprinklers requirements according to NFPA 30

Rack Sprinkler

K Factor	8	
Op. Pressure	50	Psi
Flow	56,7	gpm
Response	Quick	
Temperature	68	°C

Ceiling Sprinkler

Density	0,2	gpm/ft2
Design Area	3000	ft2
Total Flow Requirement	600	gpm
K Factor	25,2	
Op. Pressure	15	psi
Flow per Sprinkler	97,2	gpm

CFD SIMULATIONS

Performance Criteria

The evaluation of the performance of the adapted sprinklers system in the rack, will be according to the following criteria.

Flame propagation: It will be evaluated if there is presence of flames in the rack by visually verification in the simulation´s results.

Presence of combustion: By measuring the HRR it will be verified if the fire has been controlled or extinguished.

Gas Temperature: It will be verified the gas temperature produced by the fire and compared with the vaporization and/or self-ignition temperature of the liquids stored.

Sprinklers operation and water discharged*:* It will be analyzed the number of sprinklers activated and the water discharged by the system. These results will be compared with the design parameters; therefore, it will be verified if eight sprinklers are operating and if they are capable of control or extinguish the fire. In addition, the condition of ceiling sprinklers discharging 600 gpm will be validated.

Thermal radiation: The levels of thermal radiation will be analyzed to verify whether there will be ignition of materials stored in the surroundings racks.

Fire Scenarios

In the current analyzed rack, 4 bodies contain liquids that are assimilated to Ethanol and representative of the full-scale test.

The rest of the bodies in the rack contains liquids such as oil paints, water paints, etc. These liquids are outside of the scope of the analysis, due to the chemical composition is not available and the behavior against the fire is unknown, including the behavior of the vessels and cans. Therefore, the simulation of fire propagation will be in the first 4 bodies of the rack.

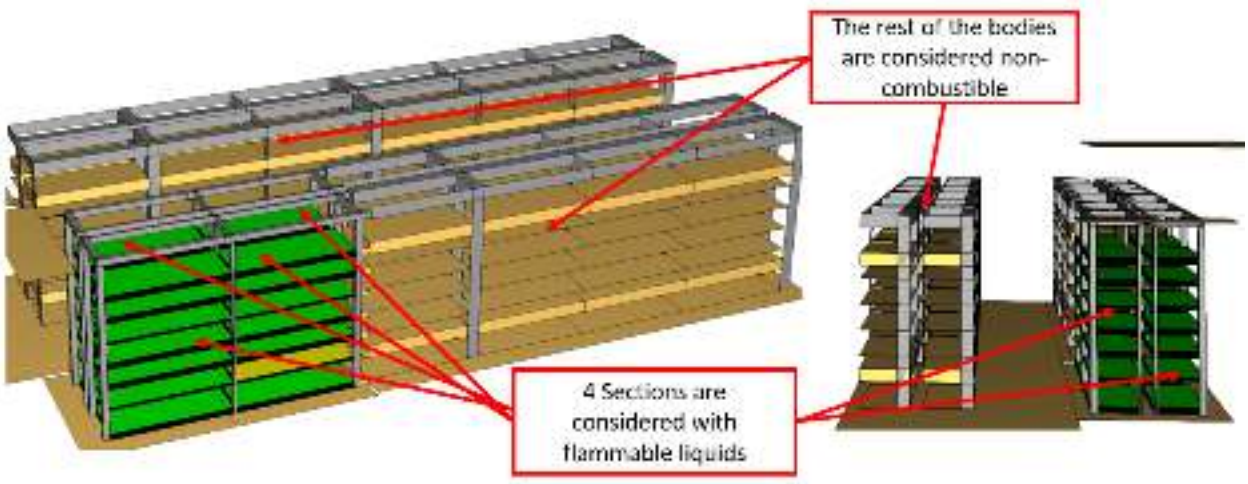

Figure 10: Arrangement of the CFD simulation

Therefore, two scenarios will be modelled. The first scenario will reflect the conditions of the full-scale test, considering the current configuration of the flammable racks in the stores. Through this scenario, is possible to review and compare the fire dynamics of the full-scale test with the CFD.

The second scenario will consider the sprinkler system adaptation, which will allow the analysis of the interaction between the sprinkler and the fire.

Assumptions and Configurations

Bleve and Jet Fires

According to the fire dynamics developed in the full-scale test, it is possible to see how the plastic bottles heat-up, therefore their internally pressure and temperature increases, losing their mechanical strength. This condition generates jet fires, spreading the fire to adjacent places and lower levels (Figure 11).

This fire condition it is not considered in the modelling due to:

- There is no information to model the mechanical deformation of plastic bottles.
- This condition increases the complexity of the model.
- This condition exceeds the time of the study.
- The consideration of this condition does not have a significant impact on the objectives of the fire modeling, due to it is intermittent and lasts less than 2 seconds.

Figure 11: Fire Behavior in the full-scale test

Fire Spreading

Regarding to the fire spreading and due to the liquids are stored in plastic bottles, the hot gases and the thermal radiation from the fire must first melt the bottles to ignite the flammable liquid inside of the bottles. In the Figure 12 (left) it is possible to see the bottles before the fire test and the bottles after the fire (right).

Figure 12: Left, bottles before fire – Right, bottles after fire

This condition is particularly complex to model and significantly increases the computational costs of the model. In addition, the interaction between the plastic containers and the fire has a negligible impact on the global development of the fire, because it only contributes in the developing of the jet fires during less than 3 seconds (Figure 13 - left).

Therefore, for the fire modelling all the metal trays in the rack are assumed to contain flammable liquid (ethanol) already spilled. This condition considers the probable worst scenario an also generates a simplified model, due to does not cover the negligible behavior of the plastic bottles for the global fire developing (Figure 13 - right).

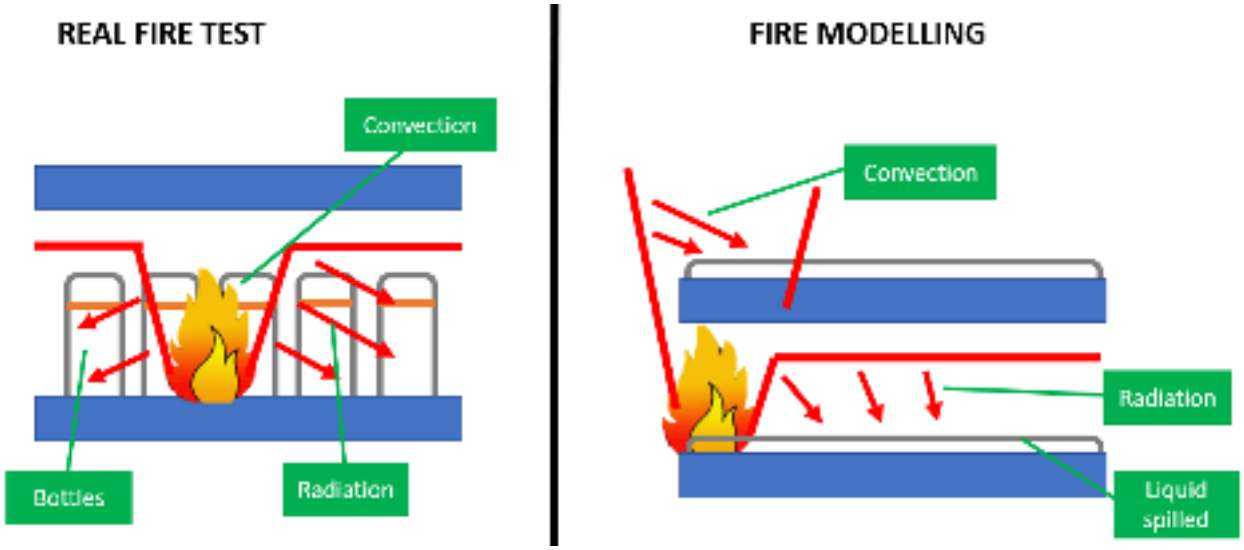

Figure 13: Fire behavior of the bottles in real fire test (left), and modelled (right)

Fire Ignition

In the full-scale test an open flame (torch lighter) has been used as an ignition source for the fire in the liquid rack. For the fire simulation, an ignition particle at 1000°C has been configured and positioned at the same place where the fire in the full-scale test was lit.

To represent the real behavior, the ignition particle has been configured through a timer deactivation, which will disable the particle after 10 seconds since the simulation start.

Fire Combustion

The substances used in the fire modeling correspond to Ethanol (fuel) and water (sprinklers). Thus, their properties are tabulated within the FDS information (Table 4). Only the ID is specified and then FDS will use pre-compiled data to calculate the several thermo-physical properties from 0K to 5000K.

Table 4: Characteristics of substances used in the fire modelling

Species	Mol. Wt. (g/mol)	Chemical Formula	σ (Å)	ε/k (K)	Liquid	RadCal Surrogate
ETHANOL	46.068440	C_2H_5OH	4.530	362.6	Y	METHANOL
WATER VAPOR	18.015280	H_2O	2.641	809.1	Y	WATER VAPOR

The complex pyrolysis model has been used to represent the free burning and the interaction between the fire and sprinklers. The CO yield and Soot yield has been considered as shown in the Table 5, while in the Table 6 the thermo-mechanical characteristics used for the Ethanol are shown.

Table 5: CO and Soot Yield

Material	ΔH_r (kJ/g)	χ_{CO_2}	χ_{CO}	χ_{Si}	χ_s	ΔH_{vb}	ΔH_{bm}	ΔH_{mt}
		(g/g)				(kJ/g)		
Ethyl alcohol	27.7	1.77	0.001	0.001	0.008	25.6	19.0	6.5

Table 6: Thermo-mechanical characteristics

Combustible	**Ethanol**	
Density	794	kg/m3
Cp	2,44	kJ/ (kg °K)
Heat of Vaporization	837	kJ/kg
Heat of Combustion	27474	kJ/kg
Thermal Conductivity	0,17	W/ (m °K)
Radiative Fraction	0,25	
Boiling Temperature	78,5	°C

Fire Extinguishment

The interaction between the fire and the sprinklers requires information that allows to model the fire extinguishment and the droplets. Thus, the autoignition temperature assigned to the Ethanol correspond to 360°C, allowing that the fire spread will be controlled by the simulation and therefore, will be not prescribed within the FDS input algorithm.

Table 7: Ethanol

Sprinklers System

According to the tests and research conducted by the WPI, it was found that running FDS with more particles per second than the default (5000) does not improve the prediction of the bucket test for a K=5.6 sprinkler. Therefore, in the current fire modelling an amount of 5000 droplets per second will be used.

For fire suppressing in shelf storage items, it is useful to consider the water droplets moving horizontally along the bottom of a solid object. This phenomenon is complex to model precisely because involves surface tension, porosity, surface absorption and the geometry of the storage. Nevertheless, the parameter ALLOW_UNDERSIDE_PARTICLES=.TRUE. is configured, to capture this phenomenon.

To assess the droplet diameter, is possible to consider the volume median diameter Dv 50, which is the diameter defined in the way that half of the volume of the water is contained in droplets with a diameter less than Dv 50 (therefore, half of the water is contained in droplets with a diameter greater than Dv 50).

According to the study and tests carried out by David Sheppard, different sprinklers with similar characteristics than the ones considered in the current research has been tested and measured, indicating Dv50 droplet size between 700 to 1000 μm.

The mathematical correlation that estimates a sprinkler droplet size is the following:

$$\frac{Dv_{50}}{D_n} = CW_e^{-1/3}$$

Where Dv_{50} corresponds to the mean value of the droplet discharged by the sprinkler, D_n correspond to the diameter of the sprinkler, C is the constant that depends on the sprinkler, which ranges from 1.74 to 3.21 and W_e is the Weber number. The Weber number is calculated according following formula.

$$We = \frac{\rho_l * U_j^2 * D_n}{\sigma}$$

Where ρ_l corresponds to the density of the water, σ corresponds to the surface tension, U is the speed of the water discharged by the sprinkler. Applying the correlations before, the droplet size (Dv50) is calculated and shown in the Table 8.

Table 8: Estimation of sprinkler droplet size

In Rack Sprinklers		
Density	1000	kg/m3
Surface Tension	0,0728	N/m
Dn	20	mm
	0,02	m
Sprinkler Surface	0,00031415	m2
Sprinkler Flow	56,7	gpm
	3,5721	L/s
	0,0035721	m3/s
Water Velocity	11,370683	m/s
Weber Number	35520	
Dv50	0,00152106	m
	1,52105915	mm
	1521,05915	um

Celling Sprinklers		
Density	1000	kg/m3
Surface Tension	0,0728	N/m
Dn	25,4	mm
	0,0254	m
Sprinkler Surface	0,00050669	m2
Sprinkler Flow	97	gpm
	6,111	L/s
	0,006111	m3/s
Water Velocity	12,060568	m/s
Weber Number	50750	
Dv50	0,00171512	m
	1,71511967	mm
	1715,11967	um

The OFFSET (m) parameter corresponds to the spherical length of atomization that surrounds the sprinkler, and where the water droplets are initially positioned in the simulation. It is assumed that after the offset, the droplets are being transported separately of each other (Figure 14).

A typical offset value of 0.01m and 0.02m is considered for the simulation, which is typically used in water sprinklers.

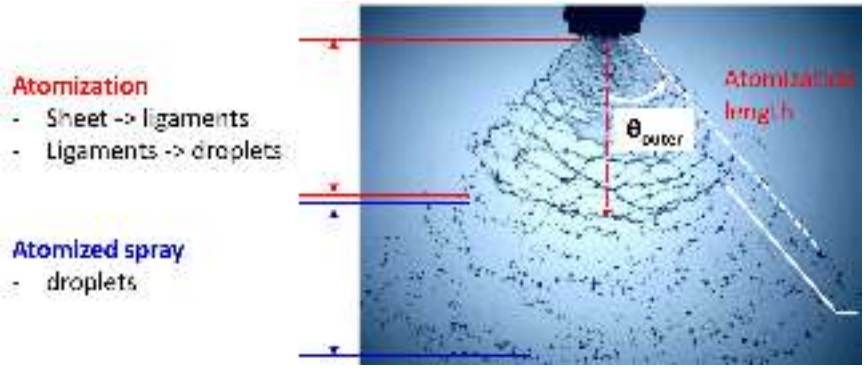

Figure 14: Atomization length (Offset)

Thus, in the Table 9 it is shown the technical information of the sprinklers (by the manufacturer) and it is included the droplet diameter estimated before.

Table 9: Sprinklers characteristics according to the manufacturer

In Rack Sprinkler		
Droplet Diameter	1520	um
Activation Temperature	68	°C
RTI	25	(m*s)^1/2
Offset	0,01	m
Water flow	214,6	L/min
Droplet Velocity	11,3	m/s
Cone Angle	75°	
Droplet per second	5000	
K Factor	8	US

Ceiling Rack		
Droplet Diameter	1715	um
Activation Temperature	74	°C
RTI	50	(m*s)^1/2
Offset	0,02	m
Water flow	366	L/min
Droplet Velocity	12	m/s
Cone Angle	85°	
Droplet per second	5000	
K Factor	25,2	US

Solids and Obstructions

The solids and obstructions in the simulation correspond to the metal trays that contain the liquids and the structure of the rack. It is not important for this study to determine the heat transfer in the elements of the rack structure; therefore, they have been considered as inert.

On the other hand, it is considered the heat transfer in the metal trays that contains the fuel. The thermomechanical properties of steel are indicated in the Figure 15, with density in kg/m3, thermal conductivity in w/(m*°k) and cp in kj(kg*°k).

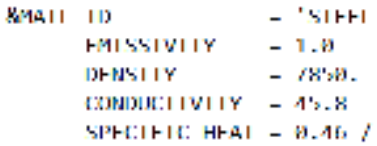

Figure 15: Thermomechanical properties of metal trays

RESULTS & DISCUSSION

Sensitivity Analysis

Simulations dominated by buoyant-force plumes, a measure of the quality of flow resolution is given by the following expression, where D* is the characteristic fire diameter and δx is the nominal cell size.

$$\frac{D^*}{\delta x} \rightarrow D^* = \left(\frac{\dot{Q}}{\rho_\infty C_p T_\infty \sqrt{g}}\right)^{\frac{2}{5}}$$

The value of Q corresponds to the total rate of heat released from the fire convectively (kW), while the denominator of the equation is the ambient density (1.2 kg/m3), the specific heat at constant air pressure (1 kJ/kg°K), the ambient temperature (293 °K) and the acceleration of gravity (9.81 m/s2).

The following cell size criterion will be used, where 4 correspond to the biggest cell size without significantly affecting the simulation results. On the other hand, the 16 correspond to the smallest cell size without demanding a high cost of computational resources.

$$4 < \frac{D^*}{\delta x} < 16$$

The methodology indicated by the SFPE to estimate the HRR of a metal tray (1m x 2.5m) will be considered. The fuel contemplated correspond to Ethanol.

$$Q = m'' \Delta H_{c,eff}\left(1 - e^{-k\beta D}\right) A_{Dike}$$

Where Q corresponds to the HRR of the pool fire (kW), m'' is the mass burning rate of fuel per unit surface area (kg/m2-sec), $\Delta H_{c,eff}$ is the effective heat of combustion of fuel (kJ/kg), A_{Dike} = surface of the pool fire (m2), $k\beta$ = empirical constant (m-1) and D = diameter of the pool fire.

Table 10: Parameters for HRR calculation

m''''	0,015	kg/m2-sec
$\Delta H_{c,eff}$	26800	kJ/kg
A_{Dike}	2,5	m2
$k\beta$	100	m-1
D	1,8	m

Therefore, the sensitivity analysis regarding the size of the cells in the areas close to the fire and where combustion occurs is shown in Table 11. It is possible to see the indicator D*/ δx is analyzed on 3 sizes of mesh (Coarse, Fine, Re-fined).

Table 11: Cell sizes according to sensitivity analysis

Mesh type	HRR (kW)	D*	Cellsize (m)	Cellsize (mm)	D*/ δx
Coarse	1000	0,6094	0,08	80	8
Fine	1000	0,6094	0,0625	63	10
Re-fined	1000	0,6094	0,04	40	15

A sensitivity analysis regarding the fire temperature has been developed to review the mesh quality. In the Figure 16 is presented the configuration of the temperature measurements and the results for both configurations.

It is possible to conclude that the differences on the measurements are neglectable in the centerline of the fire, while they start to be underestimated according to the measurement goes further from the centerline of the fire (radial T° measurement).

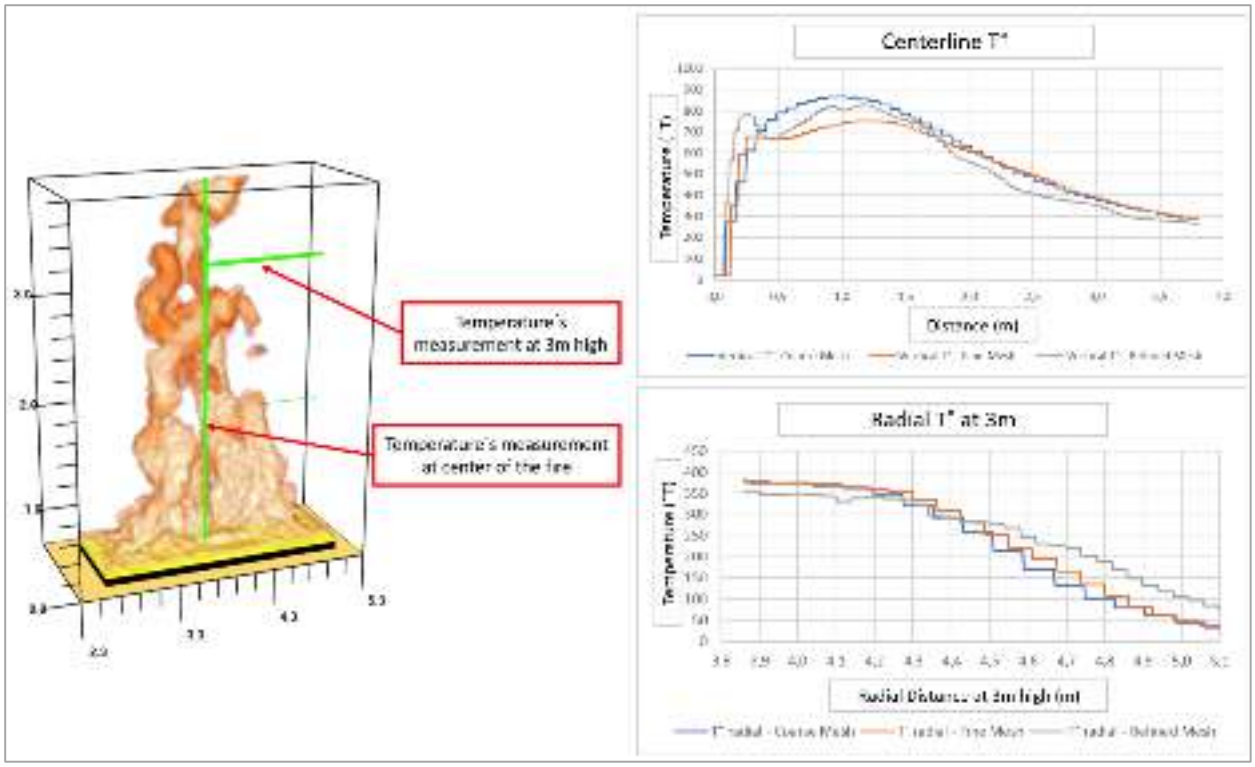

Figure 16: Temperature measurements according to sensitivity analysis

A sensitivity analysis regarding the water flow density has been developed to review the mesh quality. In the Figure 17 it is presented the measurement configuration for the water flow density and the results for the cone center. It is possible to conclude that after 4 seconds of activated the sprinkler, there is an overestimation on the water measure in the coarse mesh.

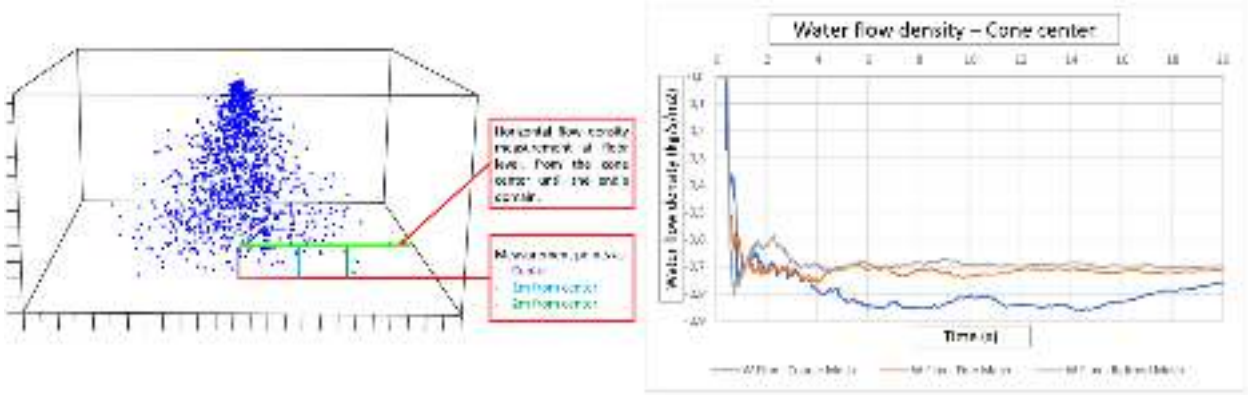

Figure 17: Organization of measurements points (left) – Results for water flow density in the cone center (right)

In the Figure 18 is possible to conclude that the coarse mesh overestimates the discharged water flow density for the first 6-8 seconds. The Figure 19 exhibits the results for the Z plane at the ground level, regarding to the water flow density in the three different cell sizes.

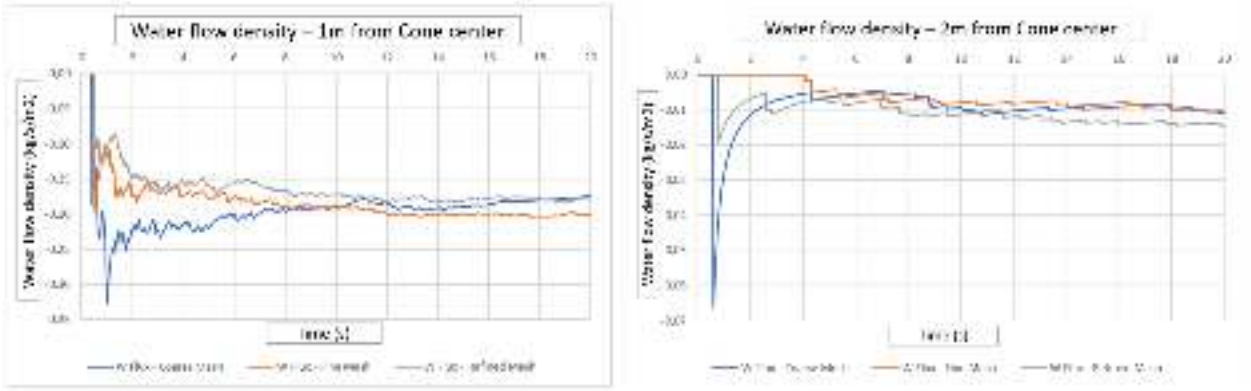

Figure 18: Results for water flow density - 1m from cone center (left) – 2m from cone center (right)

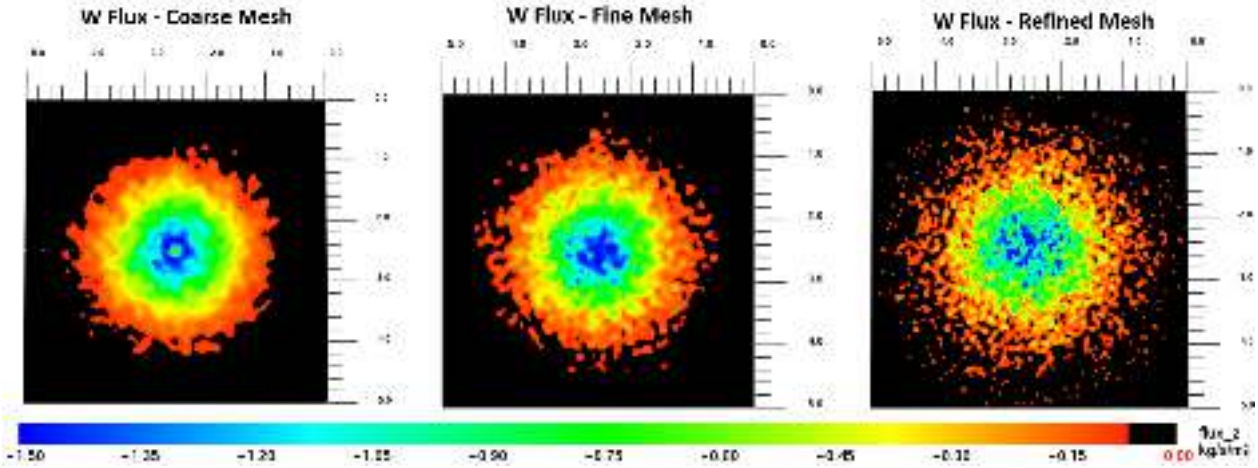

Figure 19: Z plane at the ground level – water flow density

Therefore, the cell size that correspond to the "Fine mesh" will be chosen to assess the simulations, according to the results obtained in the sensitivity analysis.

This selection is due the coarse mesh overestimates the value of the water flow density in contrast with the fine and refined mesh. The fine and refined mesh presents negligible differences, thus, the fine mesh does not require a significant computational resource (compared with re-fined mesh) to deliver accurate results.

Model Validation

To validate and verify the fire modelling, the simulation results have been evaluated with the fire dynamics of the full fire scale test. In the Figure 20 is compared the ignition time on the full fire scale test (left) and the modelling (right).

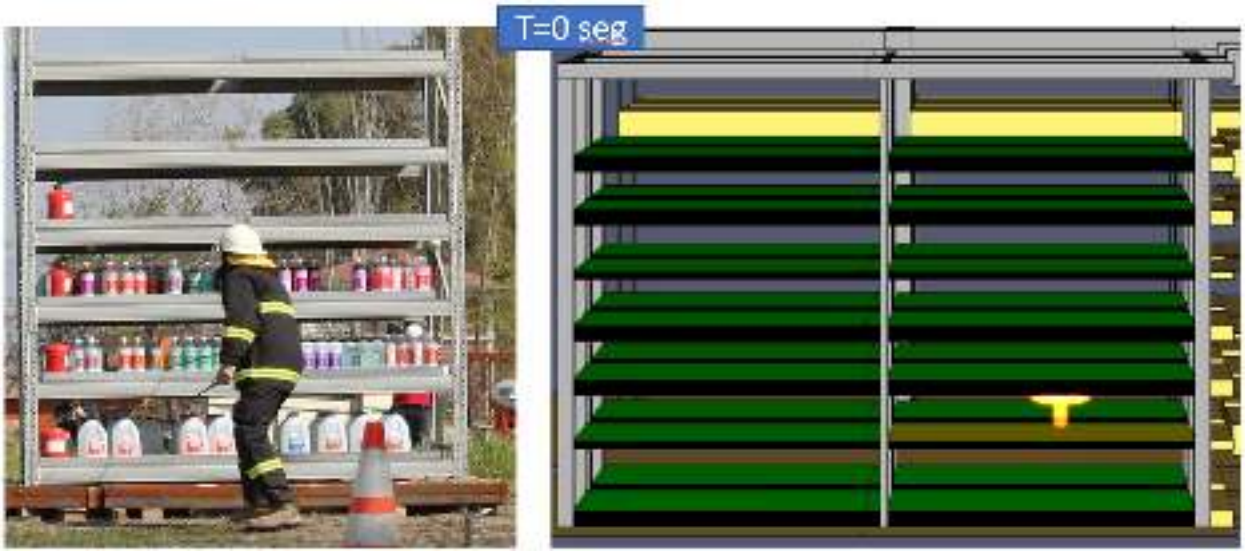

Figure 20: Fire Ignition

The Figure 21 presents the fire behavior after 3 seconds of the fire ignition in the full fire scale test (left) and the modelling (right). It is possible to point that the fire behavior and the fire spreading performs in similar structure.

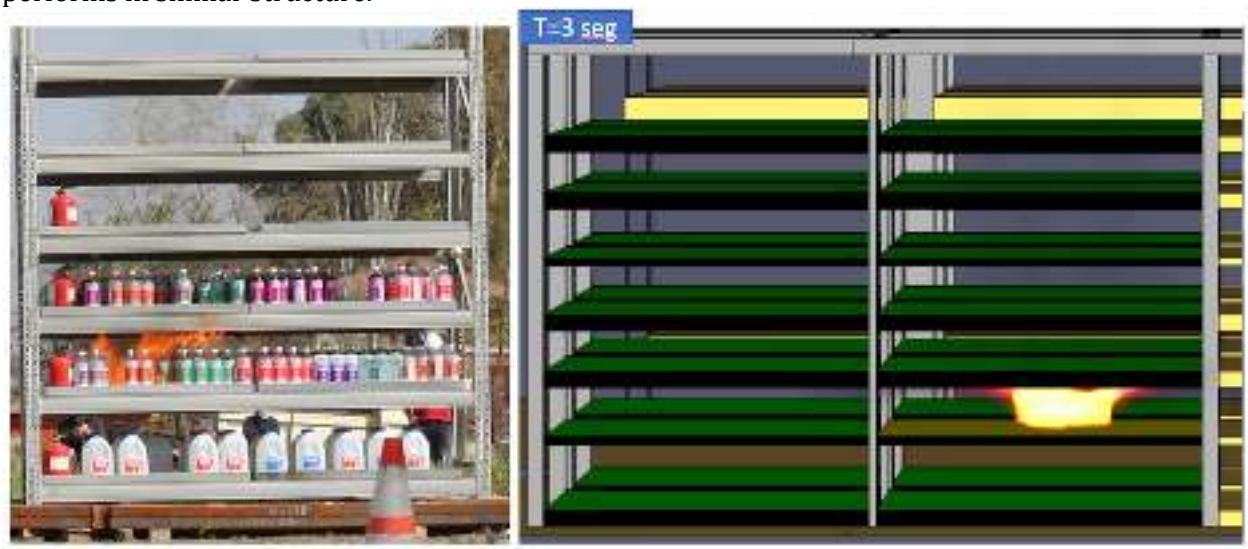

Figure 21: Fire development after 3 seconds

The Figure 22 shows the evolution of the fire after 10 seconds after the fire ignition, where in the simulation the flames have spread vertically faster than in the full fire scale test.

The reason is due to the simulation does not consider the plastic bottles, considering that the liquid is already spilled in the metal trays. On the other hand, in the full-scale test it is possible to see the activation of the dry chemical system, which influences the fire spreading.

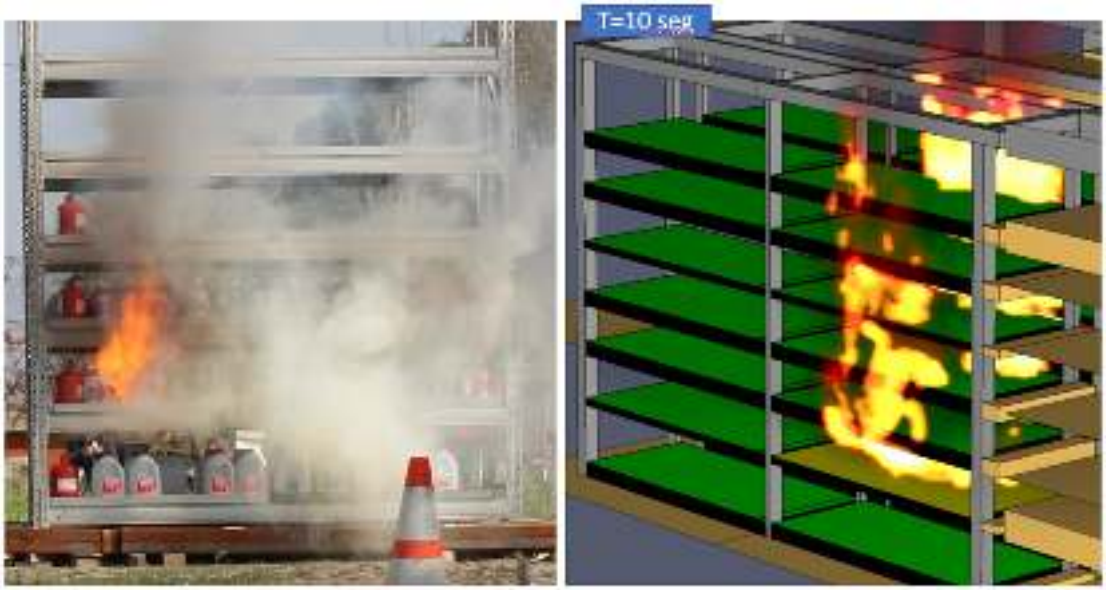

Figure 22: Fire development after 10 seconds

The Figure 23 present the evolution of the fire 12 seconds after ignition. The flames in the full fire scale test have spread vertically. On the other hand, the simulation present flames that have spread over the upper metal trays.

The vertical propagation is superior in the simulation because the plastic bottles are not considered. In addition, in the full fire scale test only 3 metal trays were used (1 above and 1 below the ignition metal tray), while in the simulation all the trays with fuel were considered. Consequently, the fire spreading is superior in the simulation.

Figure 23: Fire development after 12 seconds

The Figure 24 present the fire full scale test and modelling after 15 seconds from the ignition. The fire spreading in the simulation is superior to the fire spreading in the full-scale test. It's possible to indicate that the fire propagation begins to be similar between the fire full scale test and the simulation, due to the flames in full fire scale test exceed the height of the rack with only two metal trays burning, while in the simulation, the flames almost reach the ceiling considered the entire rack full of fuel.

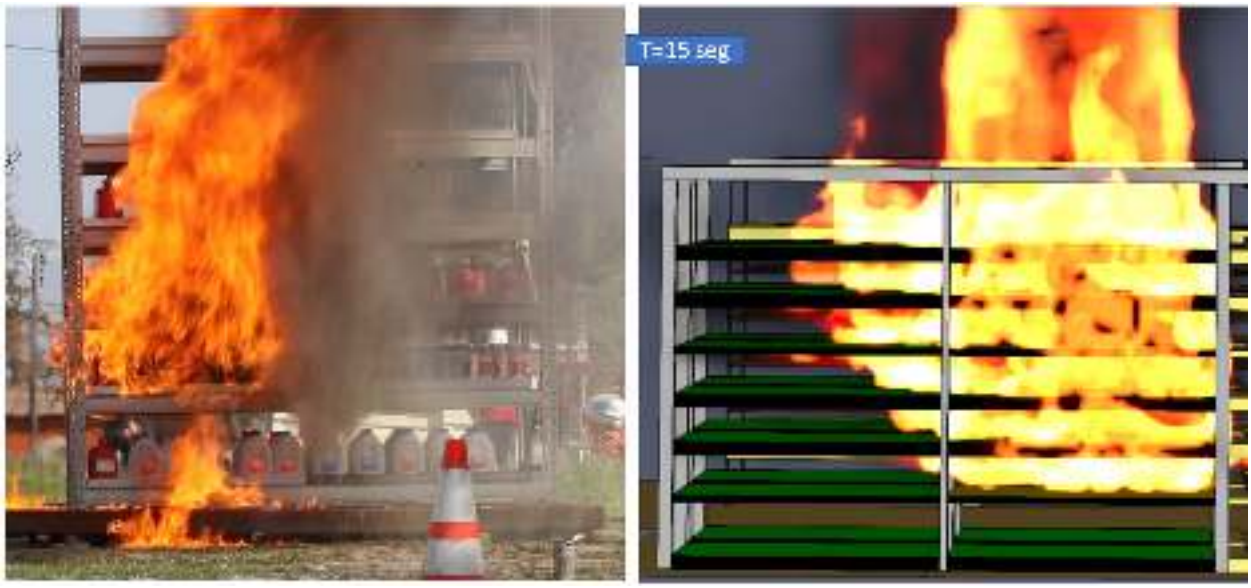

Figure 24: Fire development after 15 seconds

The Figure 25 and Figure 26 presents the fire spreading at 20 seconds and 30 seconds after the ignition of the fire. For both time intervals, the flames have spread throughout the entire rack, presenting flame height that exceeds the rack height. The horizontal fire spreading is fully developed, presenting flame sizes in the test like the simulation.

Figure 25: Fire development after 20 seconds

Figure 26: Fire development after 30 seconds

Sprinklers System Performance

Results

The Figure 27 present the time at which the first sprinklers activate. It is possible to see that both sprinklers correspond to the flue sprinklers, which ones are located between the metal trays.

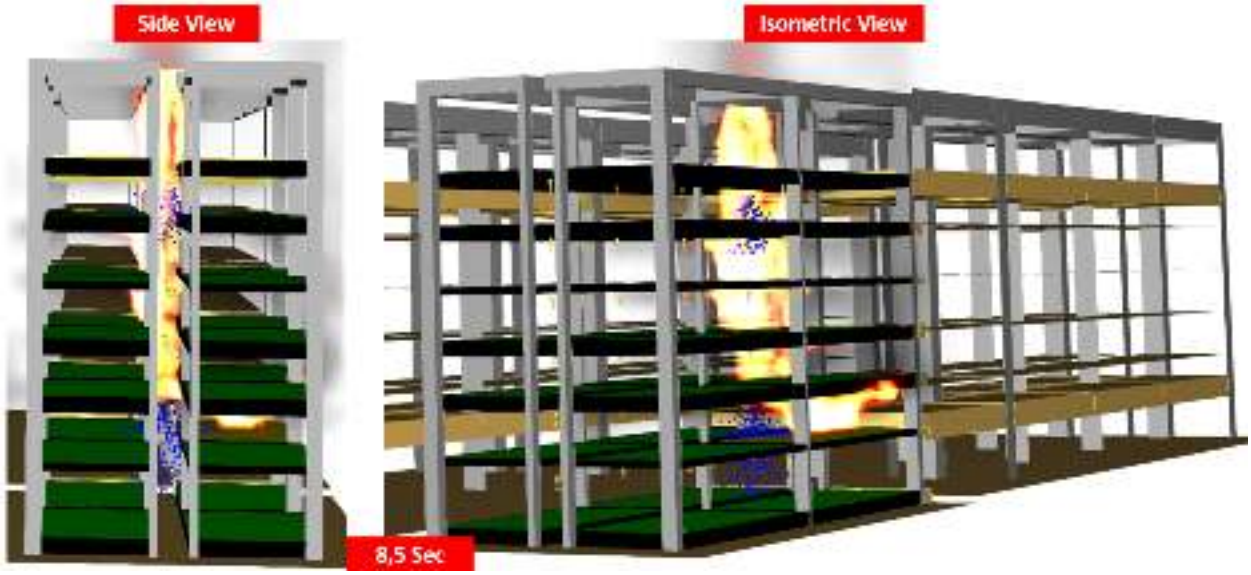

Figure 27: Simulation after 8.5 seconds from ignition

The Figure 29 exhibits the operation of the sprinklers system after 12 seconds from the ignition of the fire. It is shown that 7 more sprinklers have activated in different locations, such as sprinklers under the metal trays and flue sprinklers.

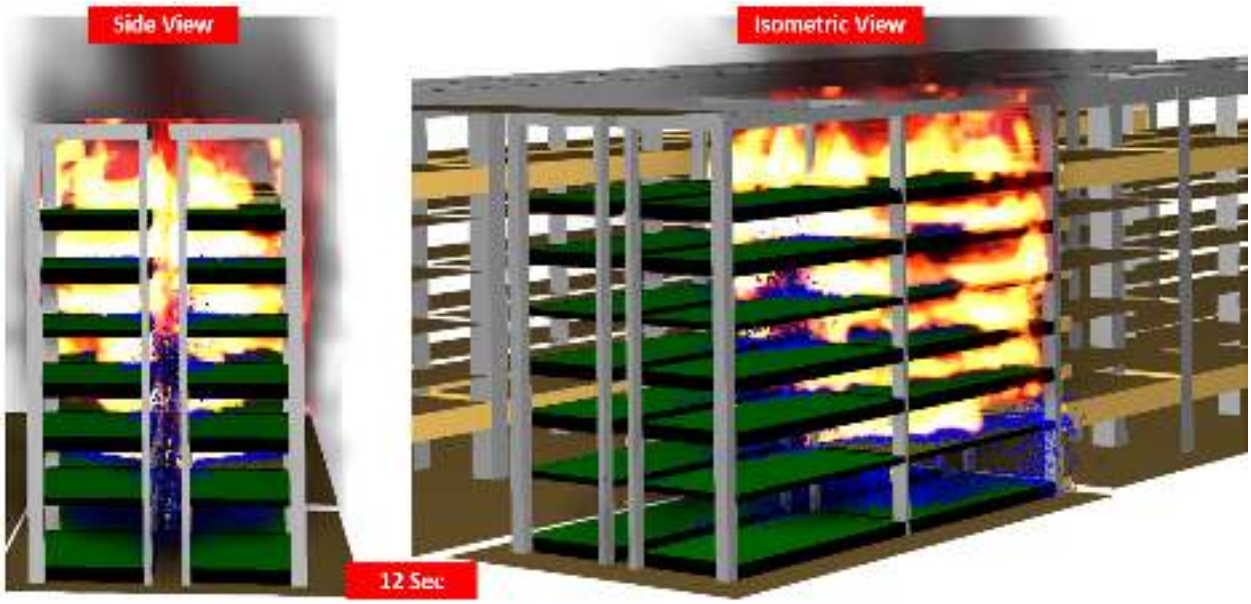

Figure 28: Simulation after 12 seconds from ignition

The Figure 29 presents the activation of the first sprinkler in the roof, which one occurs after 15 seconds of the fire ignition.

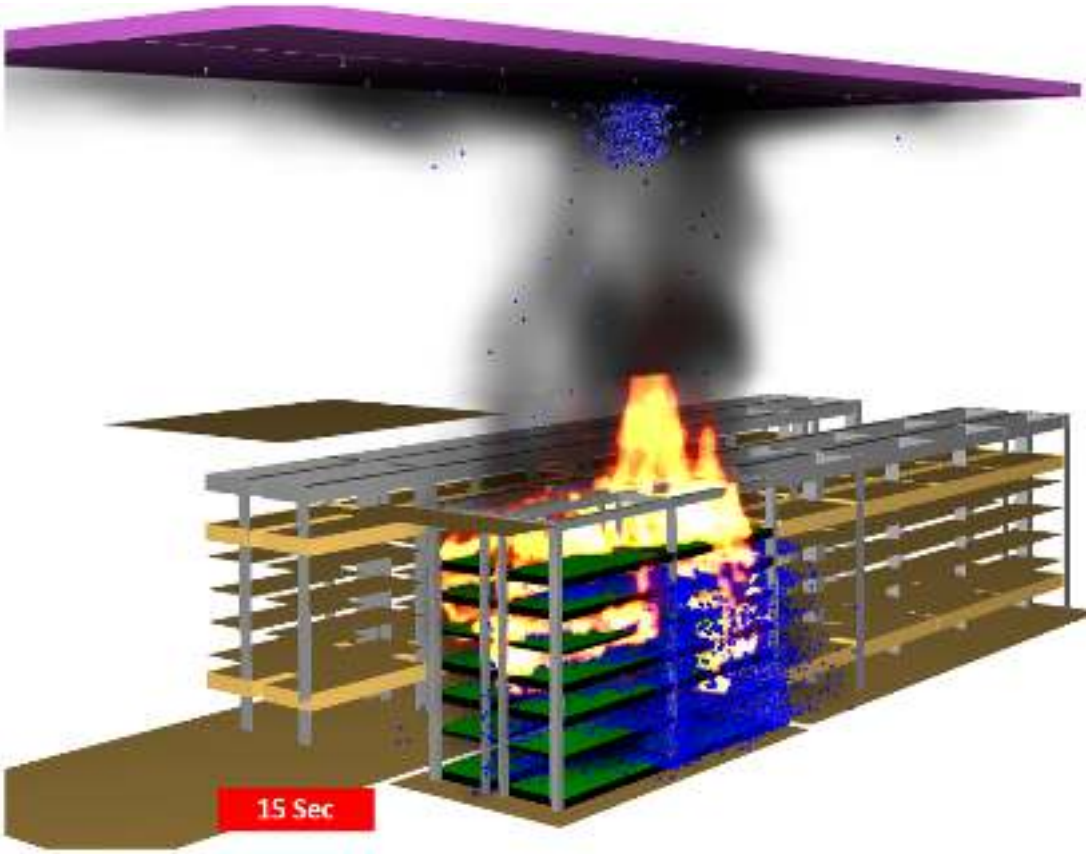

Figure 29: Simulation after 15 seconds from ignition

The Figure 30 exhibits the fire behavior and the sprinkler system operation after 20 and 40 seconds from the fire ignition. At this time interval, 8 sprinklers in the ceiling and 24 sprinklers in the rack have operated.

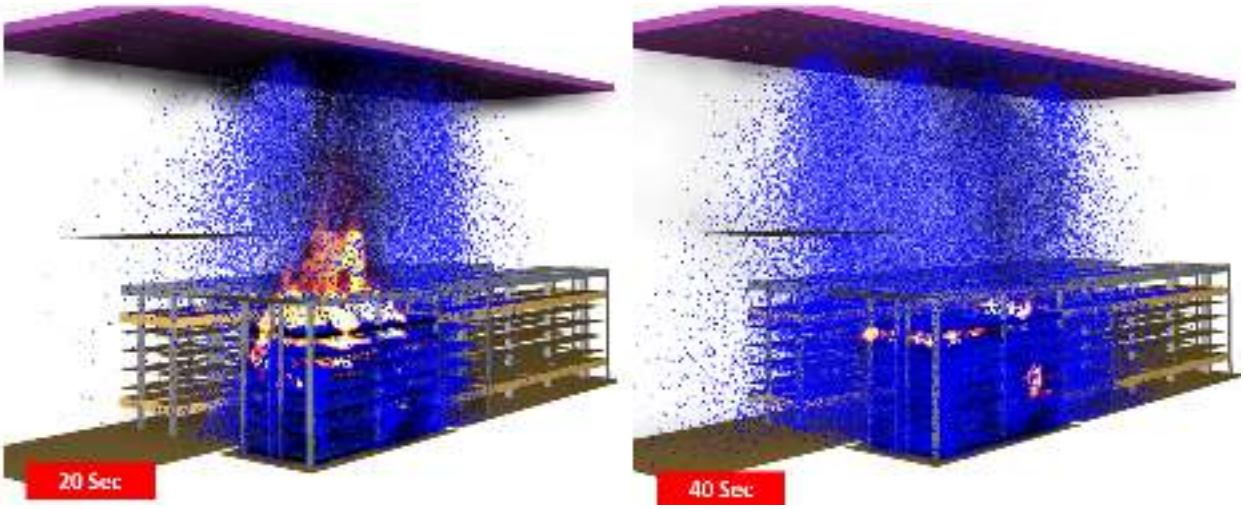

Figure 30: Simulation after 20 and 40 seconds from ignition

The Figure 31 presents the interaction between the fire and the sprinklers system for the time interval of 75 and 100 seconds after the ignition of the fire. It is possible to conclude that the fire stays steady in the HRR development, and the number of sprinklers operated remains as 8 sprinklers in the ceiling and 24 sprinklers in the rack. Therefore, the fire it has not been extinguished despite the operation of 8 ceiling sprinklers and 24 in rack sprinklers.

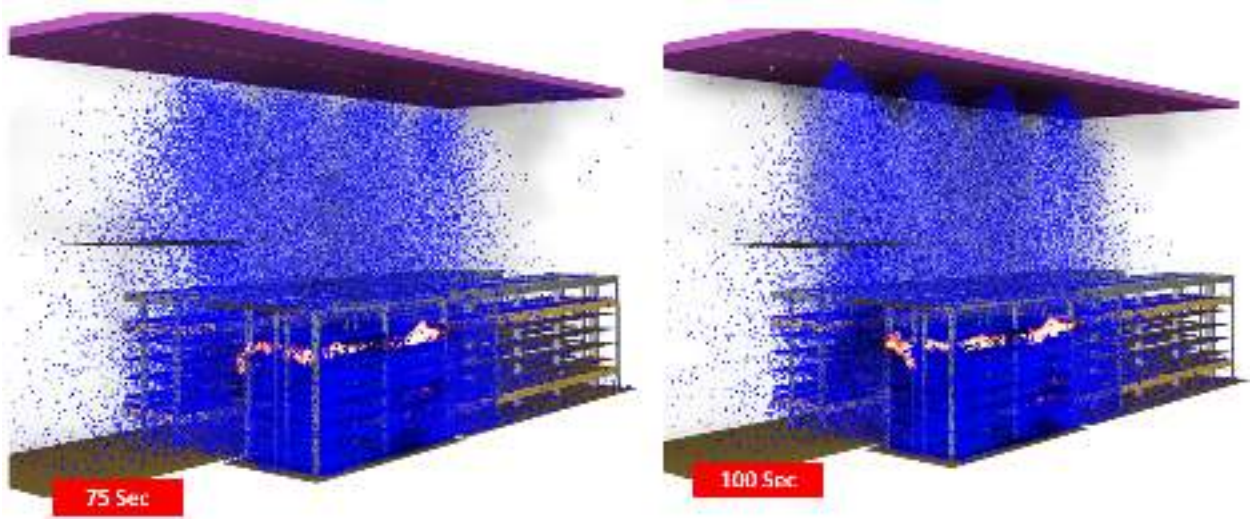

Figure 31: Simulation after 75 and 100 seconds from ignition

Analysis

In the Figure 32 is presented the HRR developed by the fire in the rack without the sprinklers system and with the sprinklers system. It is possible to conclude that the HRR is decreases in almost ten times, but the fire it is still not extinguished. The HRR of the fire controlled by the sprinklers present an average value of 4MW, which is similar than a car in a road tunnel, therefore the remaining HRR still can present a highly risk condition for the facility, structure, and occupants.

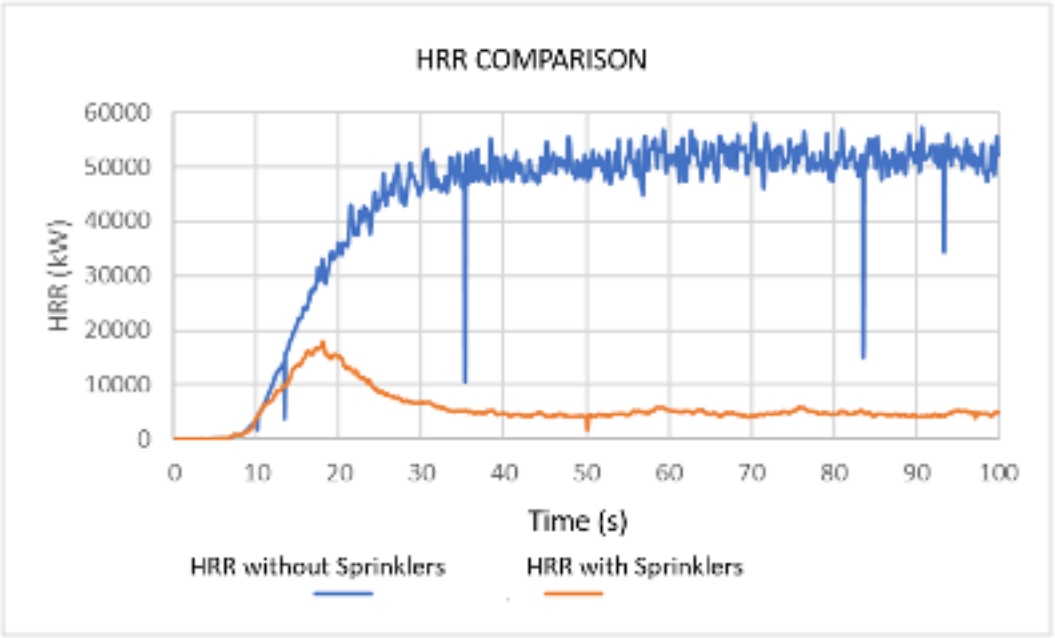

Figure 32: HRR curves

Regarding the operated sprinklers, in the Figure 33 is possible to see the timeline where quantity of sprinklers open. The first sprinkler in the rack open after 8 seconds and the last one after 37 seconds. On the other hand, the first sprinkler in the ceiling open after 16 seconds and the last after 25 seconds.

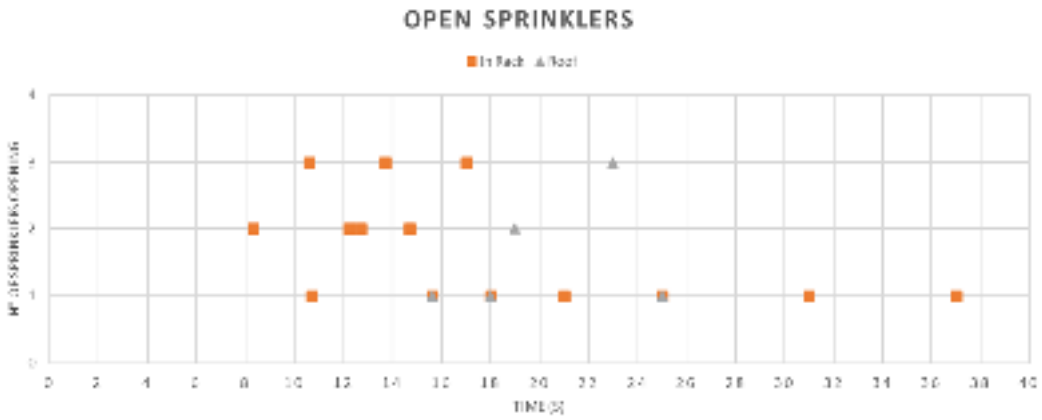

Figure 33: Sprinkler Activation

In the Figure 34 is presented an accumulated graph of the activated sprinklers and the HRR in the timeline. The maximum amount of in rack sprinklers activated correspond to 24 and occurs after 37 seconds of the ignition of the fire. On the other hand, the maximum ceiling sprinklers open correspond to 8 and take place after 25 seconds after the beginning of the fire.

It is possible to indicate that the opening curve of the in-rack sprinklers increases at same rate than the HRR. Due to the in-rack sprinklers are not capable of controlling the fire, the hot gases reach the roof and therefore the sprinklers in the ceiling start to operate, contributing to decrease the HRR.

The HRR curve begin to decrease when the ceiling sprinklers start to operate and becomes steady state after the last ceiling sprinkler and in-rack sprinkler operates after 35 seconds. Therefore, it is possible to indicate that the ceiling sprinklers are important in the control or extinguish of a fire in a storage rack.

Figure 34: Accumulated sprinklers operation and HRR curve

It is important also to notice that the first sprinklers (2) operate at 8 seconds after the ignition of the fire. At this time, the HRR developed correspond to 1.8 MW. This value is considerable high for a fire developed in 8 seconds and under the protection of a sprinklers system. The Figure 35 contain a comparison of the fire simulation with the sprinkler system and the fire full-scale test after 8 seconds from the ignition, where the fire developing present a similar behavior.

Figure 35: Comparison of Fire Simulation (Left) and Real full-scale test (Right)

Regarding with the operation of the sprinklers systems, the Table 12 presents the theoretical flow required by NFPA 30 and the measured flow discharged by the simulation. It is possible to indicate that the water discharged in the rack is 300% more than the water required by the code. Besides, the water discharged by the ceiling sprinklers is 133% more than the code´s requirements.

Table 12: Spriklers and Flow Rate

Flow required by NFPA 30

Activated Sprinklers		Flow per Sprinkler (gpm)	Flow Total (gpm)
In Rack	8	56,7	453,6
Roof	6	97,2	583,2
Hose Stream (gpm)			250
System Total Flow (gpm)			**1286,8**

Flow discharged by the CFD simulation

Activated Sprinklers		Flow per Sprinkler (gpm)	Flow Total (gpm)	% Difference from NFPA 30
In Rack	24	56,7	1360,8	300
Roof	8	97,2	777,6	133
Hose Stream (gpm)			250	0
System Total Flow (gpm)			**2388,4**	

The behavior described earlier is presented in the following set of images (Figure 36, Figure 37, Figure 38) and is visually evident that the rack sprinklers are not capable of controlling and/or reducing the HRR of the initial phase of the fire. Therefore, the hot gases developed are transported vertically and operating the ceiling sprinklers. The water discharged from ceiling starts to interact with the top of the fire (upper metal trays) and reaches the base of the fire.

As the fire continues to develop, the ceiling sprinklers continue to operate because the hot gases have not cooled down enough to prevent sprinkler operation. As more sprinklers operate, more water is discharged onto the rack and therefore it is possible to see that the fire is beginning to be controlled.

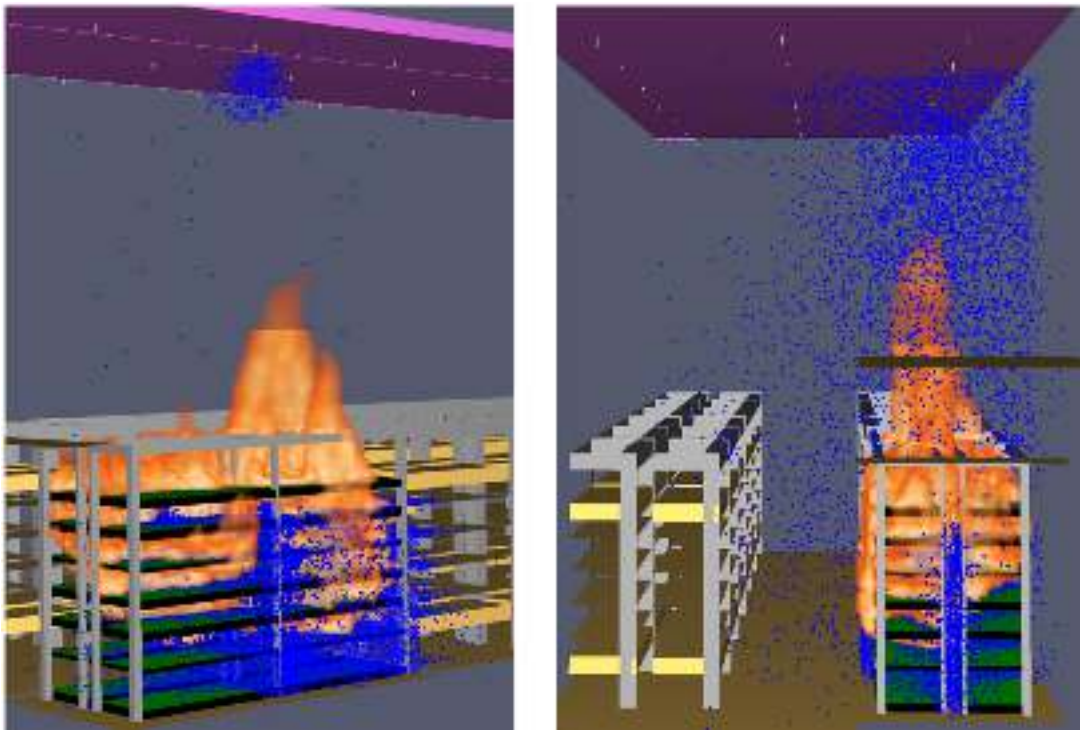

Figure 36: Interaction between ceiling sprinklers and fire

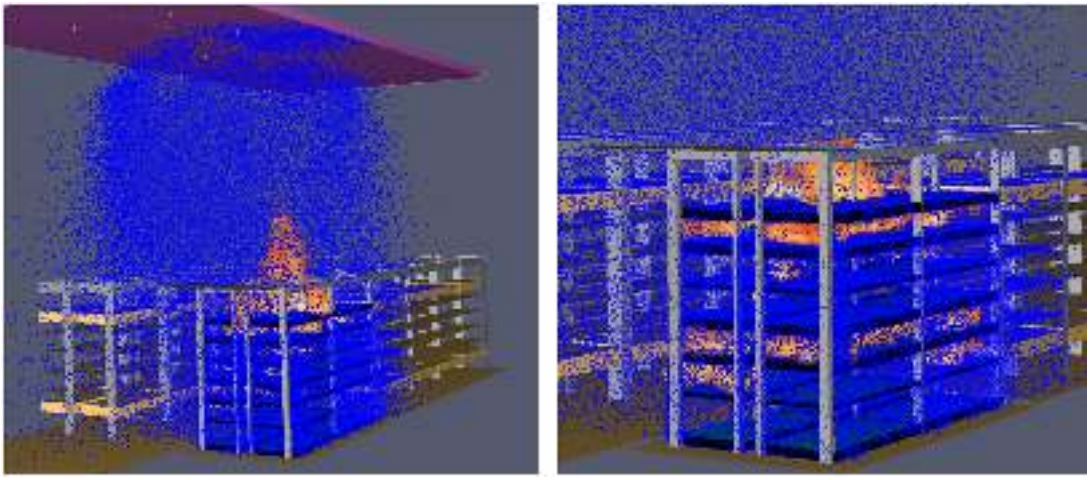

Figure 37: Continuous interaction between the sprinklers and the fire

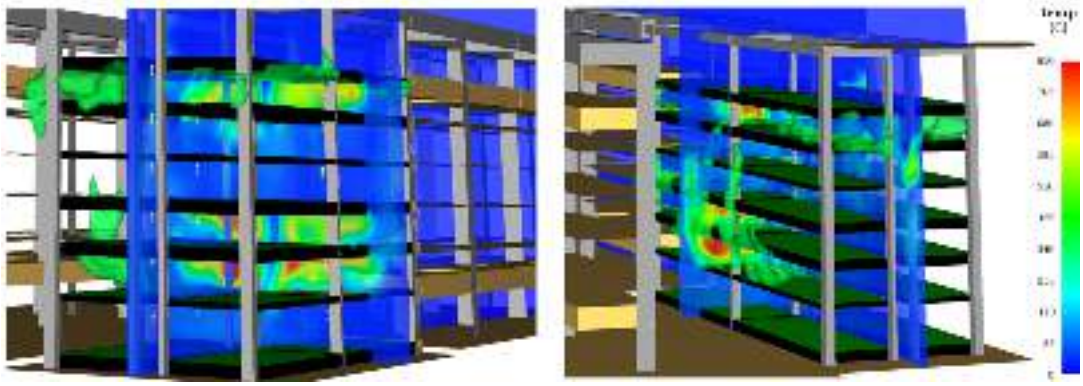

Figure 38: Gas Temperatures in the rack

Therefore, it is possible to argue that the phenomenon of skipping is presented in the system arrangement. The skipping of sprinklers occurs when a sprinkler activates significantly sooner than a neighboring sprinkler that is closer to the fire plume. Skipping reduces the amount of water delivered to the fire and therefore reduces the effectiveness of the sprinkler to extinguish the fire.

It is generally believed that sprinkler skipping is caused by the impingement of entrained and diverted droplets from previously operated sprinklers. It is reasonable to suggest that the introduction of obstructions could cause sprinkler skipping. Obstructions located near the sprinkler can redirect or change the characteristics of the water droplets such that the droplets are unable to penetrate the fire plume, and more are likely to be entrained and transferred to an adjacent sprinkler. Unfortunately, it is challenging to establish the cause of sprinkler skipping experimentally.

Skipping has the consequence of creating a region that receives a lower density of sprinkler water discharge, resulting in less effective fire control and the increased fire growth in this area. This additional fire growth results in a greater number of sprinklers operating and therefore a greater amount of water (higher density) is needed from adjacent sprinklers to control the larger fire. The overall impact of this condition requires a higher density or area of operation at the facility.

NFPA 13 provides the minimum and maximum spacing for the different types of sprinklers. It is just as important to recognize the minimum spacing requirements as the maximum spacing requirements to prevent the cold solder and skipping of adjacent rings of sprinklers in the event of a fire.

The design criteria used for the installation of fire sprinkler systems are generally developed from large-scale fire tests, where there are clear and robust requirements for the plastic containers that contains combustible and flammable liquids.

The Figure 40 present the requirements for the plastic containers. According to the NFPA 30 Handbook, very thin-walled plastic containers, such as those used for many consumer products and not intended for reuse, should not be used for routine and repeated storage of flammable products and combustible liquids. On the other hand, NFPA refer to high-density polyethylene plastic gasoline cans that are ubiquitous today. They are quite sturdy for the uses intended, being of thick-wall construction, and are approved by most jurisdictions for storing petroleum products (Figure 40).

(2) Plastic or metal containers meeting the requirements of and used for petroleum products within the scope of one or more of the following specifications:

(a) ASTM F 852, *Standard Specification for Portable Gasoline Containers for Consumer Use*

(b) ASTM F 976, *Standard Specification for Portable Kerosine and Diesel Containers for Consumer Use*

(c) ANSI/UL 1313, *Standard for Nonmetallic Safety Cans for Petroleum Products*

(d) ANSI/UL 30, *Standard for Metal Safety Cans*

(e) ANSI/UL 1314, *Standard for Special Purpose Metal Containers*

(f) FM Global *Approval Standard for Safety Containers and Filling, Supply, and Disposal Containers* — Class Number 6051 and 6052

Figure 39: NFPA 30 Requirements for containers (Left) – Examples of plastic containers according NFPA 30 (Right)

The fire spreading towards the materials stored next to the fire is highly probable. The reason is that the hot gases reach temperatures of 400°C, affecting the mechanical properties of the plastic bottles, which ones decreases between 160°C-240°C (Figure 40).

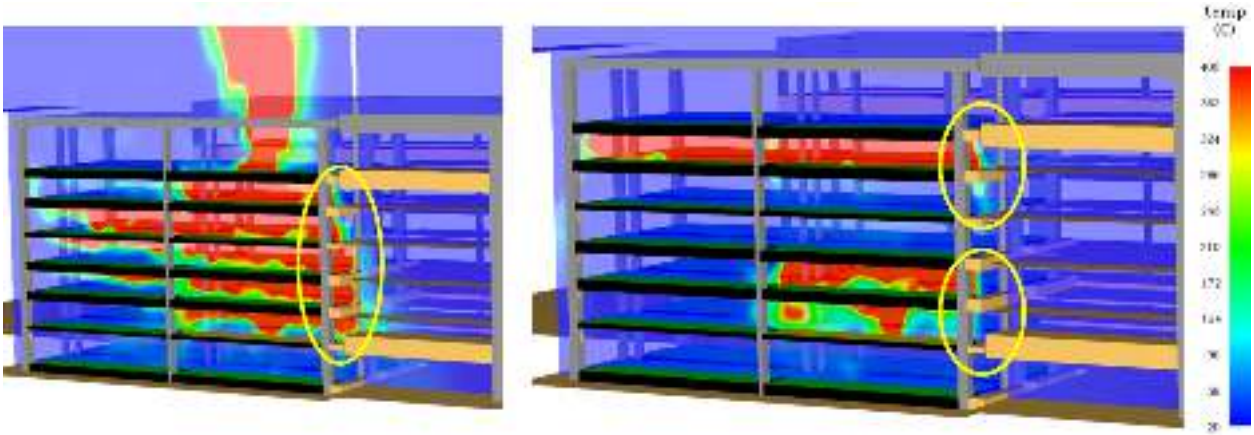

Figure 40: Convective temperature in the vicinity rack

Regarding to the thermal radiation to the adjacent racks, it is possible to conclude that the water discharged decrease the level of radiation that is received for the adjacent products. Therefore, the discharge of water creates a protecting layer for the liquids and the products stored in the contiguous racks (Figure 42). The adjacent racks receive a maximum of 2.5 kW/m2 with no sprinkler operating, while the radiation received with water discharged reach a maximum value of 0.8 kW/m2.

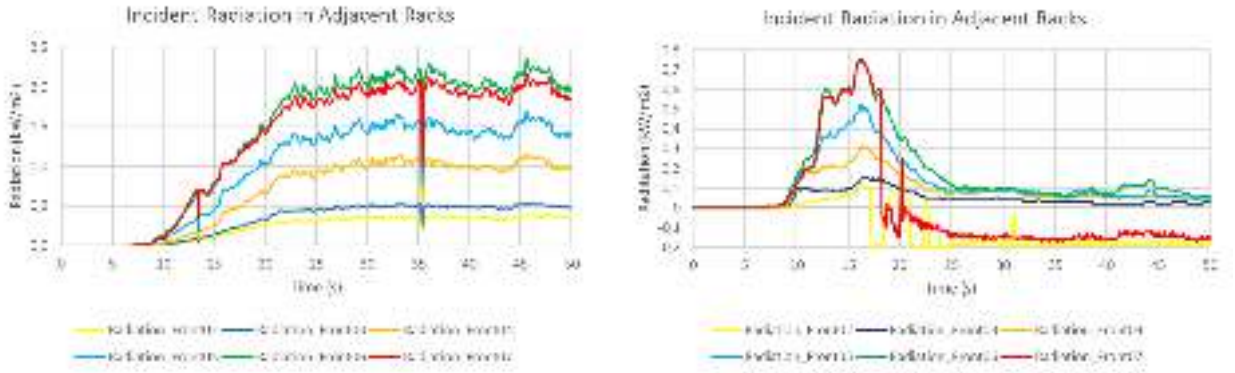

Figure 41: Thermal radiation without sprinklers (left) – Thermal radiation with sprinklers (right)

CONCLUSIONS

Regarding the fire modelling

- The simulated fire scenarios estimate and represents complex physicochemical processes; therefore, they have been consciously simplified to obtain relatively fast and reliable results. The results of this modelling/simulation correspond to an approximation of the real phenomenon.

- The modelling/simulation considers only the first 4 bodies of the rack filled with Ethanol, representing the characteristics of the rack sales in stores. The rest of the racks store liquids such as oil paints, water paints, among others. They were not considered in scope of this analysis, because:

    - They are highly difficult to represent in a computational model.
    - Their chemical composition is not available.
    - Their fire behaviour is unknown, including the containers such a bottles or metal cans.

- According to the analysis between fire validation and the full-scale test, the plastic bottles delay the ignition of the flammable liquids in the early stage (growth phase of the fire). After two or more metal trays have caught a fire, the fire development in the whole rack is independent of the plastic containers.

- The rupture of the plastic bottles due the fire was not modelled. The complexity of this phenomenon increases the computational costs of the model. Therefore, is considered that all the fuel is immediately available (all the metal trays are spilled with Ethanol), without the delay produced by the break of the plastic bottle.

As a general analysis

- The proposed adaptation of the sprinkler system according NFPA 30 standard, does not extinguish the fire. The proposed system can control the fire, reducing the HRR to an average value of 4 MW (assimilable to a light vehicle in a tunnel), which it's still a "considerable" high value for a fire inside of a store.

- The impossibility of extinguish the fire is due to the rapid propagation of the flames generated by the non-compliance of the bottles according NFPA 30.

- The fast spreading due the thin wall bottles produces the effect of skipping (random operation) in the sprinkler system.

- The water discharged by the in-rack sprinklers is 300% more than the theoretical (NFPA 30) flow required to control or extinguish a fire.

- The geometry and the bottle´s construction are main factors to control or extinguish a fire in a storage/sale rack of flammable liquids, protected by a sprinklers system.

REFERENCES

David Thomas Sheppard. (2002). “Spray Characteristics of Fire Sprinklers”. Northwestern University Mechanical Engineering Department Evanston, IL 60201.

Garner A. Palenske, Garth N. Ornelas. (2020). “Obstructions and Early Suppression Fast Response

Kevin McGrattan, Simo Hostikka, Randall McDermott, Jason Floyd, Craig Weinschenk, Kristopher Overholt. (2017). “Fire Dynamics Simulator User’s Guide”. NIST Special Publication 1019 Sixth Edition

Matthew J. Klaus. (2013). “NFPA 13 Automatic Sprinkler Systems Handbook”. Twelfth Edition. National Fire Protection Association Quincy, Massachusetts.

Morgan J. Hurley. (2016). “SFPE Handbook of Fire Protection Engineering”. Fifth Edition

Robert P. Benedetti, Paul E. May. (2012). “NFPA 30 Flammable and Combustible Liquids Code Handbook”. National Fire Protection Association Quincy, Massachusetts.

Sprinklers”. Fire Protection Research Foundation 1 Batterymarch Park, Quincy, MA 02169.
Ning Ren, Andrew F. Blum, Ying-Hui Zheng, Chi Do, And André W. Marshall. (2008). “Quantifying the Initial Spray from Fire Sprinklers”. Department of Fire Protection Engineering University of Maryland, College Park, MD, USA.

Tarek Beji & Bart Merci. (2016). “Fluid Mechanics Aspects of Fire and Smoke Dynamics in Enclosures”. Department of Flow, Heat and Combustion Mechanics, Ghent University, Ghent, Belgium.

Topi Sikanen & Simo Hostikka. (2016). “Modeling and simulation of liquid pool fires with in-depth radiation absorption and heat transfer”. Fire Safety Journal 80 (2016) 95–109.

Yi Wang, Karl V. Meredith, Xiangyang Zhou, Prateep Chatterjee, Yibing Xin, Marcos Chaos, Ning Ren, And Sergey B. Dorofeev. (2014). FM Global, Research Division Norwood, MA 02062, USA.